Journal of Reproductive Immunology 92 (2011) 33–44

Contents lists available at SciVerse ScienceDirect

Journal of Reproductive Immunology

journal homepage: www.elsevier.com/locate/jreprimm

Systemic inflammation, cellular influx and up-regulation of ovarian VCAM-1 expression in a mouse model of polycystic ovary syndrome (PCOS)

María Emilia Solano[a,*], Valeria Analía Sander[b], Hoang Ho[c], Alicia Beatriz Motta[d,1], Petra Clara Arck[a,1]

[a] *Laboratory for Experimental Feto-Maternal Medicine, Department of Obstetrics and Fetal Medicine, University Medical Center Hamburg-Eppendorf, Martinistr. 52, 20246 Hamburg, Germany*
[b] *Instituto de Investigaciones Biotecnológicas-Instituto Tecnológico de Chascomús (IIB-INTECH), UNSAM-CONICET, Chascomús, Buenos Aires, Argentina*
[c] *Brain-Body-Institute, Department of Medicine, McMaster University, Hamilton, Ontario, Canada*
[d] *Laboratory of Ovarian Physiopathology, CEFYBO-UBA-CONICET, Buenos Aires, Argentina*

ARTICLE INFO

Article history:
Received 17 June 2011
Received in revised form 7 September 2011
Accepted 23 September 2011

Keywords:
PCOS
Metabolism
Chronic inflammation
Ovary
Adhesion molecules

ABSTRACT

PCOS, a major cause of anovulatory sterility, is associated with obesity, insulin resistance and chronic inflammation. New evidence suggests that the immune system aggravates the clinical features of PCOS. Our aim was to study the immune, metabolic and endocrine features of a mouse model of PCOS elicited by androgenisation using dehydroepiandrosterone (DHEA). We observed a significant weight gain and insulin resistance in DHEA-androgenised mice, coupled with the formation of ovarian follicular cysts. DHEA up-regulated the expression of vascular cell adhesion molecule (VCAM)-1 and intercellular adhesion molecule (ICAM)-1 in the granulosa cell layer of the majority of cysts, and VCAM-1 expression in the theca cell layer of all follicles and cysts. The expression of these markers was low in control tissue. Peritoneal cells from PCOS-mice showed enhanced production of inflammatory cytokines, suggesting an association between chronic inflammation and PCOS. In addition, DHEA-androgenisation induced the activation of $CD4^+$ cells both *in vivo* and *in vitro*, and their expression of the respective ligands for VCAM-1 and ICAM-1, VLA-4 and LFA-1, as assessed *in vitro*. $CD4^+$ cells were present in androgenised ovaries, especially in the granulosa cell layer of cysts with high VCAM-1 expression. Herein, we present novel evidence that the immune system is activated systemically and locally in a mouse model for PCOS. We propose that VCAM-1 is involved in aggravating PCOS symptoms by promoting leukocyte recruitment to the ovaries and perpetuating local inflammation. These findings offer novel therapeutic opportunities for PCOS, such as blockage of VCAM-1 expression.
© 2011 Elsevier Ireland Ltd. All rights reserved.

1. Introduction

Polycystic ovary syndrome (PCOS) is one of the most common endocrine disorders in premenopausal women, constituting the main cause for anovulatory infertility (Franks et al., 2008). The manifestation of PCOS is heterogeneous and complex, involving both reproductive and metabolic features. Currently, it is diagnosed if two of the following symptoms are present: polycystic ovaries, hyperandrogenism and/or ovulatory dysfunction (upon exclusion of specific disorders, i.e. congenital adrenal hyperplasia) (Rotterdam, 2004). In addition to infertility, women with PCOS frequently suffer from obesity (Hahn

* Corresponding author. Tel.: +49 40741058710; fax: +49 40741040183.
E-mail address: e.solano@uke.uni-hamburg.de (M.E. Solano).
[1] These authors contributed equally to this work.

0165-0378/$ – see front matter © 2011 Elsevier Ireland Ltd. All rights reserved.
doi:10.1016/j.jri.2011.09.003

et al., 2005; Martinez-Bermejo et al., 2007) and abdominal distribution of body fat, along with metabolic alterations such as insulin resistance (Hahn et al., 2005) and dyslipidaemia (Meyer et al., 2005a,b).

Despite its high prevalence (5–8%) of women during their reproductive years are affected (Asuncion et al., 2000; Azziz et al., 2004; Diamanti-Kandarakis et al., 1999; Knochenhauer et al., 1998), only very limited insights are available with regard to the pathophysiology of PCOS (as reviewed by Pasquali et al. (2011)). However, published evidence suggests that the anovulation and cystogenesis seen in PCOS patients result from alterations in the development of the ovarian follicles (Franks et al., 2008; Hughesdon, 1982; Maciel et al., 2004). To ensure normal folliculogenesis, ovulation and corpus luteum formation and regression, a fine-tuned immune response is required (Brannstrom and Norman, 1993; Bukulmez and Arici, 2000; Sander et al., 2008; Wu et al., 2004). Hence, alterations in immune cells infiltrating the ovary and of cytokines in follicular fluid – as observed in patients with PCOS (Amato et al., 2003; Gallinelli et al., 2003; Jansen et al., 2004; Omu et al., 2003; Wu et al., 2007) – may account for the onset and severity of PCOS symptoms. It is also known that several markers of systemic inflammation, such as C-reactive protein (CRP), leukocyte frequencies, pro-inflammatory cytokines (Amato et al., 2003; Benson et al., 2007; Möhlig et al., 2004; Puder et al., 2005; Sayin et al., 2003) and the soluble forms of cellular adhesion molecules (CAMs) intercellular adhesion molecule (ICAM)-1 and vascular cell adhesion molecule (VCAM)-1 (Diamanti-Kandarakis et al., 2006; Escobar-Morreale et al., 2003) are increased in women with PCOS. In addition, epidemiological data reveal that markers of early vascular dysfunction, such as arterial stiffness and carotid intimal media thickness, are associated with obesity and insulin resistance in women with PCOS (Meyer *et al*., 2005a, 2005b). Thus, low-grade chronic inflammation – along with hyperandrogenism and metabolic disorders – has been proposed to be a major risk factor for the occurrence of cardiovascular disease in women affected by PCOS (Orio et al., 2005).

Though its aetiology is not completely understood, it has been suggested that PCOS results from an intrinsic dysfunction in androgen synthesis (Escobar-Morreale and San Millán, 2007). As a cure for PCOS remains elusive, current therapies focus on targeting the prevailing symptoms in order to minimize the impact of the syndrome on quality of life and health in the long term (Goodarzi et al., 2011). Over the past years, several animal models have been developed with the intent of studying the complexity of PCOS (reviewed by Abbott et al. (2005)). Among them, hyperandrogenism provoked by application of steroid hormone dehydroepiandrosterone (DHEA) in rodents has been shown to reproduce the main clinical features of PCOS, such as ovarian cysts, anovulation and altered endocrine environment (Lee et al., 1991; Luchetti et al., 2004; Roy et al., 1962). It should be noted that mice enter estrous cycles subsequent to the discontinuation of DHEA application (Yan et al., 1997). This model has been extensively used to study ovarian and endocrine disorders, investigate pathological mechanisms and new therapies (Bas et al., 2011; Lee et al., 1998; Henmi et al., 2001; Sander et al., 2006). However, insights on metabolic parameters observed in patients with PCOS are largely elusive in DHEA-treated mice.

In the present work, we employed this model in order to study the role of the immune system in relation to major clinical aspects of PCOS pathology, ovarian dysfunction and metabolic parameters. We also aimed to test different protocols of PCOS induction in mice in order to identify which approach would reproduce the clinical symptoms of PCOS most accurately in mice. Finally, to elucidate whether the systemic and ovarian effects of DHEA administration were due to direct actions of the hormone on immune cells, we performed *in vitro* experiments in which cell phenotype as well as expression of CAMs were determined after DHEA stimulation.

2. Materials and methods

2.1. Animals and experimental protocol

New born Balb/c animals were kept with their respective mothers in an animal facility with a 12 h light/dark cycle. Water and food were available *ad libitum*. At the age of 21 days, female animals were weaned and sorted for subsequent experiments. Animal care and experimental procedures were followed according to institutional guidelines and conformed to requirements for animal research conduct in Germany and Canada.

In a group of animals, PCOS like symptoms were induced by s.c. injection of DHEA (60 mg/kg BW/day dissolved in 0.1 ml neutral oil) to 23 days old (Protocol 1) and to 30 days old females (Protocol 2) for 20 consecutive days. Age and weight matched control females received vehicle alone over a period of 20 days. The respective stage of the estrous cycle were determined daily upon obtaining vaginal smears collected over the entire course of the experiment, as described in the Supplementary methods. Body weight was assessed every 3 days during the experiment. A second group of naïve 23 days' old females was used to obtain tissue for *in vitro* experiments.

2.2. Tissue collection and cell isolation

On day 20 of DHEA or vehicle administration, animals were anesthetized by i.p. injection with a solution of 20 mg/kg ketamine and 100 mg/kg xylacine in PBS and sacrificed by cervical dislocation. Two blood samples were collected from each female. The first one was centrifuged to obtain serum for estradiol determination. The second sample was heparinized and incubated for 5 min with RBC lysis buffer (e-bioscience) in order to enrich leukocytes for flow cytometry staining. For detailed information on the protocols for estradiol determination and flow cytometry staining and on the antibodies used, consult the Supplementary methods.

Peritoneal cells were harvested by peritoneal lavage with 5 ml of PBS. Cells were washed with AimV culture medium and stimulated for cytokine production as described in the Supplementary methods.

One ovary of each animal was fixed in paraformaldehyde 4% in PBS and embedded in paraffin; the second one

was embedded in OCT media (Tissue Tek) and snap frozen in liquid N_2.

The second group of naïve 23 days old females was euthanized. Inguinal, axillar and mesenteric lymph nodes from each animal were pooled and mechanically disaggregated through a 100 μm mesh (Becton and Dickinson) in PBS.

2.3. In vitro stimulation with DHEA

Lymph node cells from naïve animals were cultured *in vitro* (37 °C, humidified atmosphere of 95% O_2: 5% CO_2) for 21 and 48 h with 0, 0.1, 1 or 10 μM DHEA in 10% FCS RPMI-1640 culture media. DHEA dilutions were prepared from a stock solution of DHEA dissolved in ethanol. After the incubations, the frequency and phenotype of cells were determined by flow cytometry assay, as detailed in the Supplementary methods.

2.4. Fasting glucose and insulin determination

In an independent experiment, animals received DHEA or vehicle, respectively, for 20 days commencing on day 23 of age. On day 20 of treatment, the females were deprived of food from 8:00 a.m. to 2:00 p.m., for 6 h (Andrikopoulos et al., 2008). Blood samples were taken to determine glucose levels in the moment by precision extra glucose strips in the Accu-check Advantage II Blood Glucose Monitor (Roche Diagnostics) and to obtain serum. Serum insulin concentrations were quantified using the Ultra Sensitive Mouse Insulin ELISA Kit (Crystal Chem Inc.) according the manufacturer's instructions. These results were used to calculate the Homeostasis Model of Assessment of Insulin Resistance (HOMA-IR) = {[fasting insulin (pM)] × [fasting glucose (mM)]}/405 (Berglund et al., 2008; Muniyappa et al., 2008) as an index of insulin resistance.

2.5. Ovarian morphology

Serial paraffin histological sections (5 μm) from the entire ovarian tissue specimen were stained for H&E and evaluated using a Zeiss Axioscope light microscope with the Zeiss KS400 software. Ovaries form both groups showed follicles in different stages of development. In rare cases ovaries from both groups presented corpora lutea. Ovarian cysts were identified as large fluid filled follicles with attenuated granulosa cell layer. Cyst frequency was determined and their histological characteristics, such as size, thickness of granulosa and theca cell layers, were quantified and compared to the largest tertiary follicle observed in each control ovary.

2.6. Immunohistochemical detection of VCAM-1, ICAM-1, CD11c, MHC-II and CD4

The staining was carried out as described before (Prados et al., 2011). Briefly, cryostat sections (8 μm) were incubated with avidin, biotin and protein-blocking solutions (Vector), followed by overnight incubation with the antibodies (Ab) against the surface antigens: MHCII, CD4, VCAM-1 and ICAM-1 (for additional information about the Ab and dilutions used, refer to Table 2 in Supplementary methods) at 4 °C in humid chamber. Sections used as negative controls followed the same protocol, but were incubated with 1% FCS in TBS (representative photos are displayed in Supplementary Fig. 2). After washing, the sections stained for ICAM-1 underwent the amplification and revealing steps. The remaining sections were incubated with biotinilated 0.5% goat anti-rat IgG Ab (Jackson Laboratories) in 4% mouse normal serum and 2% FCS in TBS for 30 min. As amplification system, we used ABC-AP (VECTASTAIN®, Vector) 1:100 in TBS for 30 min. The tissue expression of the protein of interest (CD4, MHC II, VCAM or ICAM) was unveiled using alkaline phosphatase substrate solution, which allows to identify expression of proteins of interest by its dark pink colour, followed by a light blue counterstaining with 0.1% Meyer's haematoxylin.

Slides were examined using a Zeiss Axioscope light microscope and photo documentation was performed with a digital image analysis system (Zeiss KS400). Follicular stages were differentiated as previously described (Cheng et al., 2002). Briefly, primary follicles were observed as an oocyte surrounded by a single layer of cuboidal granulosa cell, whereas secondary follicles presented the oocyte surrounded by two or more layers of granulosa cells with no antrum. Tertiary follicles were identified by the presence of a fluid-filled antrum. The theca cell layer of all the primary, secondary, tertiary and cystic follicles of every ovary and the stromal tissue was scored by the intensity of the VCAM-1 and ICAM-1 and the frequency of infiltrating $MHCII^+$ and $CD4^+$ cells. Tissue expression of the respective marker was semi-quantified as follows: 0, absence of positive signals; +, low; ++, moderate; +++, high expression. The percentage of primary, secondary, tertiary and cystic follicles per ovary presenting positive cells for VCAM-1, ICAM-1, MHCII and CD4 in the granulosa cell layer was also evaluated. In ovaries, it is difficult to identify vessels by morphological criteria, as they are often collapsed. Thus, we refrained to include them in the analysis.

2.7. Statistical analysis

Analyses were carried out using SPSS 15.0 for windows and means were compared by the Mann–Whitney *U* test. Statistical significance was set at $p < 0.05$.

3. Results

3.1. DHEA androgenisation induced the formation of cysts

Analysis of ovarian histological sections revealed that the administration of DHEA for 20 days induced the formation of 1–3 follicular cysts per ovary (Fig. 1). Cysts appeared as enlarged ovarian follicles with increased antrum and attenuated and compacted theca and granulosa cell layer. The granulosa cell layer was frequently detached to the antrum and showed evidence of cell infiltration (Fig. 1D–F). Tissue from both, control and DHEA treated female mice showed viable and atretic follicles at different stages of development (Fig. 1A, B, D and E) and no follicular cysts were observed in control ovaries (Table 1).

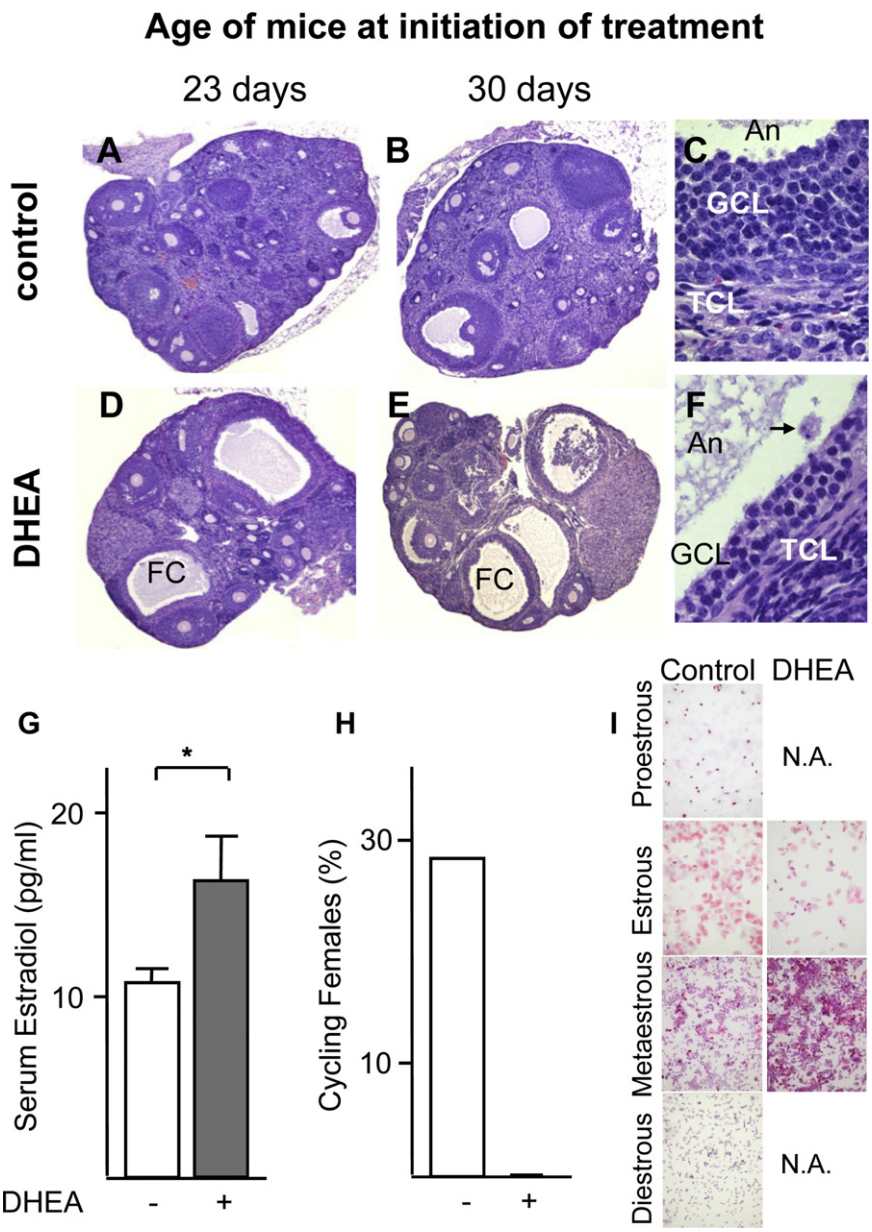

Fig. 1. DHEA androgenisation induced key ovarian features of PCOS. Photomicrographs of ovaries from control (A–C) and androgenised animals (D–F). Animals were 23 (A and D) or 30 days of age (B and E) at the beginning of DHEA injections. Control and DHEA-androgenised ovaries showed follicles at different stages of development. Androgenised ovaries also exhibited the formation of follicular cysts (FC). Representative examples of the follicular wall of a tertiary follicle (E) and of a cyst (F) show the antrum (An), theca cell layer (TCL) and granulosa cell layer (GCL). The arrow points a leukocyte in the antrum. Serum estradiol levels (G) were increased upon DHEA androgenisation. (H) Estrous cycle arrest was observed by means of the % of females exhibiting complete estrous cycles. (I) Photomicrographs of the vaginal smears from control and androgenised animals stained for H&E show examples of proestrous, estrous, metaestrous and diestrous stages, if applicable. Values are the mean ± SEM; $n = 7$. $^{*}p \leq 0.05$ control vs. DHEA-androgenised mice, Mann–Whitney *U* test. N.A., not applicable; (A, B, D and E) Magnification: 25× and (C, F and H) 200×.

Two different experimental approaches were tested for DHEA-androgenisation in order to identify the most accurate resemblance to PCOS ovarian symptoms. In the first approach, we commenced androgenisation on day 23 of age (Luchetti et al., 2004). In a novel approach, the effect of DHEA administration commencing on day 30 of age was tested. Morphological analysis of the ovaries from animals androgenised according the different protocols revealed similar morphological features. However, cysts were larger and more frequent when DHEA was administrated to mice beginning at an age of 23 days (Table 1). Hence, in subsequent experiments, we employed the approach of experimental cystogenesis induction by commencing DHEA treatment at an age of 23 days.

Table 1
Morphometric analyses of histological sections of ovarian tissue from control and androgenised animals treated according protocols 1 and 2. The values represent the mean ± SEM.

Age at initiation of DHEA treatment	23 days (Protocol 1)		30 days (Protocol 2)	
n per group	6	7	7	6
DHEA	Nil	+	Nil	+
Number (and percentage) of mice with FC development	0	7(100)	0	5(71)
Cysts per ovary	0.0 ± 0.0	2.7 ± 0.6**	0.0 ± 0.0	1.4 ± 0.4*
Thickness of TCL (μm)	18.2 ± 1.1	10.9 ± 0.9**	24.4 ± 10.4	20.7 ± 2.2*
Thickness of GCL (μm)	44.9 ± 5.2	33.2 ± 3.0	53.1 ± 4.9	33.3 ± 3.0*

* $p < 0.05$, Mann–Whitney *U* test.
** $p < 0.01$, Mann–Whitney *U* test.

3.2. Ovarian steroidogenic function is altered after DHEA administration

PCOS diagnosis in humans depends not only in the formation of ovarian cysts, as induced by DHEA in this murine model, but also in the presence of oligo- or anovulation and hyperandrogenism. To confirm the presence of these clinical features in DHEA-treated mice, we analysed serum estradiol levels as a marker for steroidogenic function and observed a significant increase in DHEA-treated mice (Fig. 1G). The altered ovarian function was independently confirmed by the absence of the normal estrous cycling, as estrous stages were limited to estrous or metaestrous upon DHEA treatment (Fig. 1H and I). In contrast, control animals began to exhibit regular cycling activity at an age of 39.3 ± 2.7 days. The formation of ovarian cysts together with the absence of ovarian cycles further strengthens that DHEA-induced PCOS-like symptoms in mice mirror pivotal clinical features of PCOS in humans.

3.3. Metabolic changes after DHEA androgenisation

Next, we investigated whether DHEA-treatment mirrors metabolic changes seen in women with PCOS. An increase in body weight could be observed in androgenised mice compared to the age-matched control mice, which reached levels of significance 17 days upon of initiation of DHEA-treatment (Fig. 2A). In addition, the androgenisation increased fasting levels of serum insulin (Fig. 2B) and blood glucose (Fig. 2C). These alterations resulted in higher values for HOMA-IR in androgenised animals, indicating increased insulin resistance compared to controls (Fig. 2D).

3.4. Markers of chronic inflammation were increased after DHEA administration

Since PCOS in humans has been linked to chronic inflammation (Benson et al., 2007), we then aimed to analyse the production of inflammatory cytokines by peritoneal immune cells in mice treated with DHEA, compared to untreated control mice. CBA analyses of the cytokine production by peritoneal cells revealed an increased production of the proinflammatory cytokines IL-12p70, TNF, IFN-γ, MCP-1 and IL-6 as well as the anti-inflammatory cytokine IL-10 (Fig. 3A–G).

3.5. Ovarian expression of cell adhesion molecules

It is well established that inflammatory processes such as cytokine changes can up-regulate the tissue expression of CAMs. Also, insulin can selectively induce VCAM-1 expression (Madonna et al., 2008). Based on the above described alterations in DHEA-treated mice, i.e. elevated serum insulin and increased cytokine production by peritoneal immune cells, we then aimed to immunohistochemically analyse the presence and localization of CAMs in the ovaries upon experimental cystogenesis induction. Strikingly, in DHEA androgenised ovaries, all the follicles as well as the cysts expressed high amounts of VCAM-1 in the theca cell layer. Furthermore, the majority of ovarian cysts expressed also VCAM-1 in the granulosa cell layer (Fig. 4B and D and Table 2). Conversely, expression of VCAM-1 was low in ovaries from control mice (Fig. 4A and C). Here, VCAM-1 expression was distributed in the theca cell layer of the follicles and – rather faint – in the stroma. In ovaries from both groups only a low percentage of secondary and tertiary follicles expressed VCAM-1 in the granulosa cell layer (Table 2).

Further, in androgenised ovaries, ICAM-1 expression could be detected in the majority of cysts expressed in granulosa cell layer (Fig. 4H and Table 2), whereas, in control and androgenised ovaries, ICAM-1 expression was low in theca cell layer of developing follicles, in granulosa cell layer of few secondary follicles and moderate in the stroma (Fig. 4E–H and Table 2).

3.6. DHEA androgenisation in vivo increases the frequency of T helper cells and natural killer (NK) cells

T helper cells can be recruited to the site of inflammation by ICAM-1 and VCAM-1. In order to study whether DHEA treatment also affects the frequency and activation status of $CD4^+$ T cells that can bind them, we analysed peripheral blood mononuclear cells by flow cytometry. We also analysed the frequency of NK cells, as a population that is generally increased in chronic inflammation processes (Brüünsgaard and Pedersen, 2003). We observed that the percentage of activated T cells ($CD4^+CD25^+$) was increased in response to DHEA, as well as the frequency of $CD4^+$ T helper cells alone, though the latter one did not reach levels of significance (Fig. 5A–C). We also observed an increase in the frequency of NK cells upon DHEA treatment (Fig. 5D

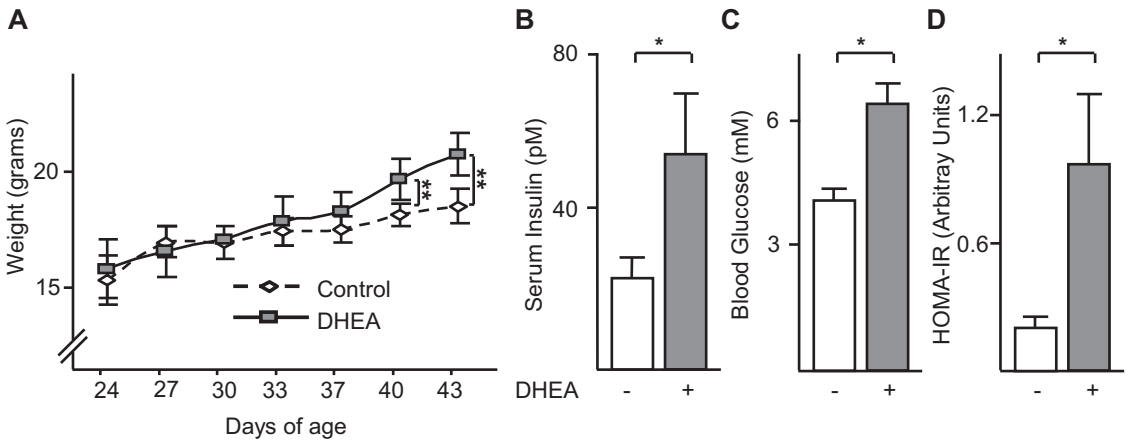

Fig. 2. Weight gain and fasting glucose and insulin levels in androgenised females. (A) Growth curves for the period of the treatment for control (open triangles) and androgenised animals (filled squares). DHEA androgenisation increased the fasting levels of insulin in serum (B) and glucose in blood (C). The calculation of the HOMA-IR (D) showed an increase in the insulin resistance. Values represent the mean ± SEM. $^{*}p < 0.05$, $^{**}p \leq 0.01$ control vs. DHEA, Mann–Whitney *U* test.

Table 2
Qualitative and quantitative analyses of VCAM-1, ICAM-1, MHCII and CD4 ovarian tissue expression.

	VCAM-1		ICAM-1		MHC II		CD4	
n per group	6	7	7	4	6	4	6	5
DHEA	Nil	+	Nil	+	Nil	+	Nil	+
TCL								
Primary Fll	N.A.	N.A.	N.A.	N.A.	N.A.	N.A.	N.A.	N.A.
Sec. Fll	+	+++**	+	+	++	++	+	+
Tertiary Fll	+	+++**	+	+	++	++	+	+
Cysts	N.A.	+++[c]	N.A.	++[c]	N.A.	++[c]	N.A.	+[c]
Stroma[a]	−/+	+	++	++	+++	+++	+	+
GCL/antrum[b]								
Primary Fll	0.0 ± 0.0	0.0 ± 0.0	0.0 ± 0.0	0.0 ± 0.0	0.0 ± 0.0	0.0 ± 0.0	0.0 ± 0.0	0.0 ± 0.0
Sec. Fll	3.0 ± 3.0	17.0 ± 12.0	3.0 ± 3.0	2.5 ± 2.5	19.4 ± 4.6	13.4 ± 6.7	9.8 ± 3.8	8.4 ± 3.6
Tertiary Fll	6.5 ± 2.7	16.2 ± 6.5	0.0 ± 0.0	0.0 ± 0.0	8.3 ± 5.2	3.8 ± 2.4	7.2 ± 5.4	16.0 ± 9.8
Cysts	N.A.	91.0 ± 9.0[c]	N.A.	100[c]	N.A.	100[c]	N.A.	100[c]

N.A., not applicable; Fll., follicles; Sec., secondary.

[a] Intensity (VCAM-1, ICAM-1) or frequency (MHC II, CD4), quantified as absent (−), low (+), moderate (++) or high (+++).

[b] Frequency of follicles positive for respective marker. The percentage of follicles presenting positive cells in the GCL was determined for each ovary and used to calculate the mean ± SEM.

[c] Due to the lack of cysts in control tissue, this result could not be compared statistically.

** $p < 0.01$, as determined by Mann–Whitney *U* test.

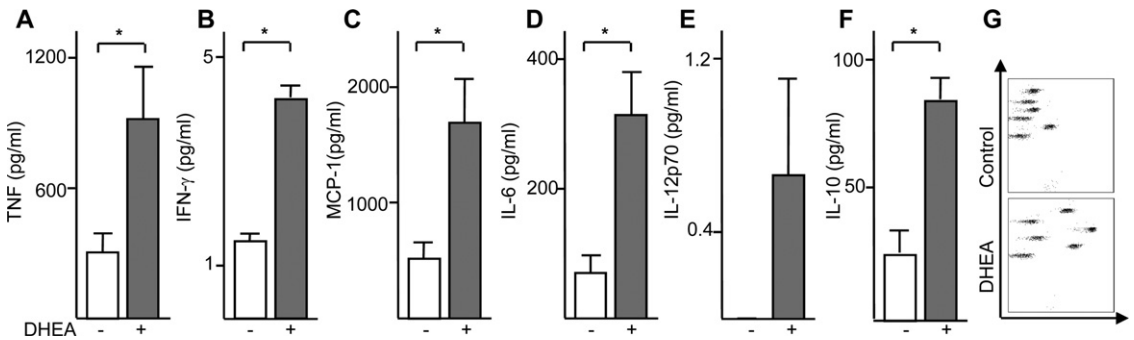

Fig. 3. Androgenisation increased the production of cytokines by peritoneal cells. The bars show the concentration of cytokines (TNF, IFN-γ, MCP-1, IL-6, IL-12p70 and IL-10, A-F, respectively) in the culture media of peritoneal cells from control and androgenised animals, as assessed by CBA. The dotplots show representative examples of the flow cytometry results obtained from control and androgenised samples. From top to bottom, the bead clouds show IL-6, IL-10, MCP-1, IFN-γ, TNF and IL-12p70. Values are the mean ± SEM, $n = 5$, $^{*}p < 0.05$, Mann–Whitney *U* test.

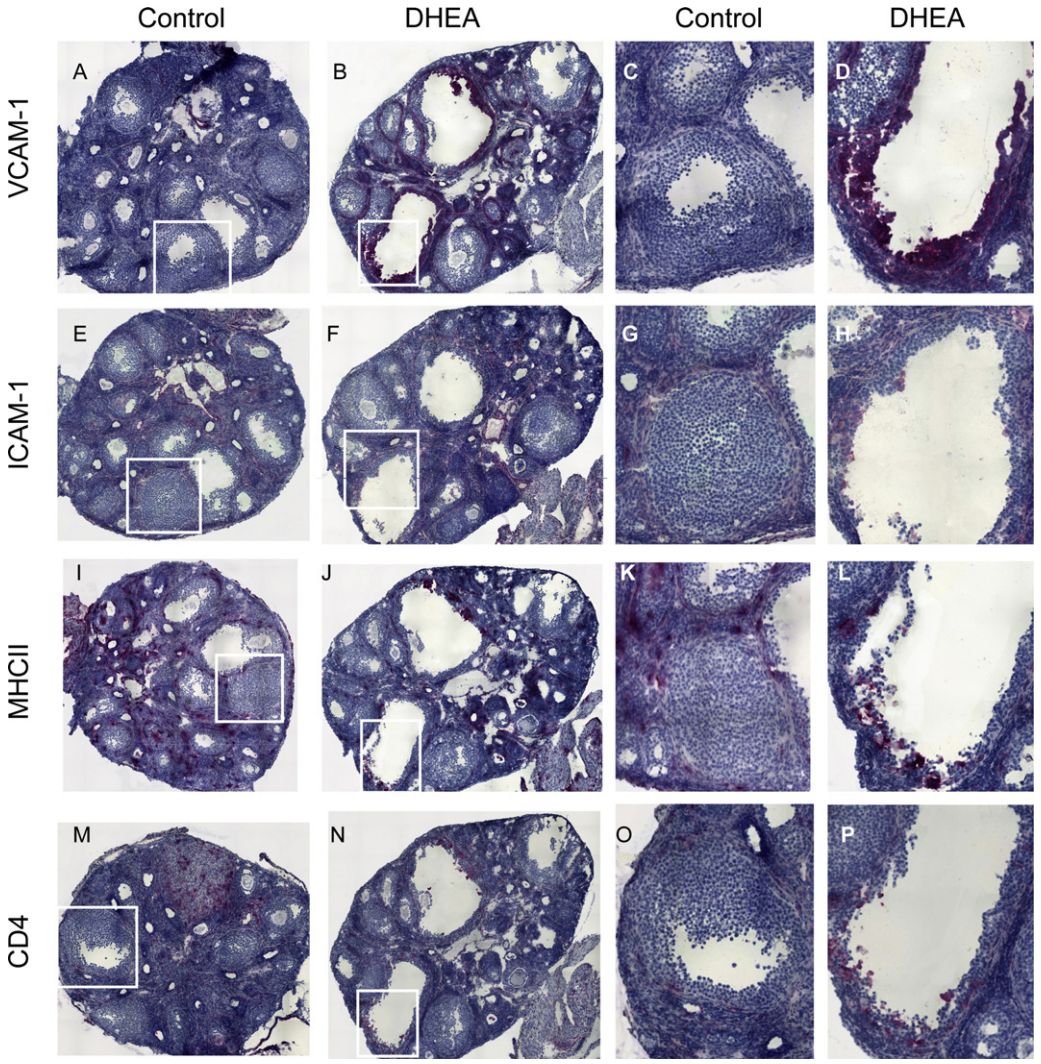

Fig. 4. Ovarian expression of VCAM-1, ICAM-1, CD4 and MHCII. Photomicrographs of ovarian tissue specimens representative for control (A, E, I, and M) and DHEA androgenised (B, F, J, and N) females, labelled for VCAM-1 (A and B), ICAM-1 (E and F), MHCII (I and J) and CD4 (M and N). The rectangles indicate the area magnified in photos shown in (C), (D), (G), (H), (K), (L), (O), and (P). Here, a tertiary follicle from control tissue is shown in (C), (G), (K), and (O) and a FC from DHEA-androgenised tissue in (D), (H), (L), and (P) upon labelling for VCAM-1, ICAM-1, MHCII and CD4, respectively. Tissue sections from DHEA treated mice revealed high expression of VCAM-1 in the TCL of follicles and cysts (B and D). The GCL and antrum of the cyst also revealed the presence of cells which could be identified as ICAM-1$^+$, MHCII$^+$ or CD4$^+$ (H, L, and P). In ovaries of control mice, expression of these markers was rarely observed in GCL of follicles and their distribution was limited to the TCL and stroma (A, C, E, G, I, K, M, and O). Magnification 25× (A, B, E, F, I, J, M, and N) and 200× (C, D, G, H, K, L, O, and P). IHC detection was revealed with alkaline phosphatase, thus, cells that are positive for the respective marker appear in pink. Tissue was counterstained with haematoxylin. Photos showing positive cells in a higher magnification and the negative controls for the staining are provided in the Supplementary files.

and E), although at a lower frequency compared to T cells. Taken together, these analyses – along with the enhanced production of inflammatory cytokines by peritoneal cells – support the association between chronic inflammation and PCOS in the mouse model employed here.

3.7. DHEA stimulation in vitro promoted the up-regulation of CAM ligands

Based on the increased activation of CD4$^+$ cells and the striking finding of the up-regulated ovarian expression of VCAM-1, we then wished to assess whether DHEA affects the VCAM-1-binding ligand, the integrin very late antigen (VLA)-4, expression in T cells. VLA-4 is normally expressed on leukocyte plasma membranes and adheres to VCAM-1 upon stimulation. Hence, we wished to test whether DHEA directly up-regulates cellular expression of VLA-4. We performed the analyses in an *in vitro* setting, as this allows analyses in a dose dependent approach and limits the effect of an indirect up-regulation of VLA-4 through, e.g. the altered steroidogenesis. Besides VLA-4, we also focused on lymphocyte function-associated antigen (LFA)-1 expression, which binds to ICAM-1. We observed that lymph node-derived leukocyte stimulation with DHEA for 21 and 48 h did not alter the overall frequency of CD3$^+$, CD4$^+$ and CD8$^+$ cells (Supplementary Fig. 1A and Table 3). However,

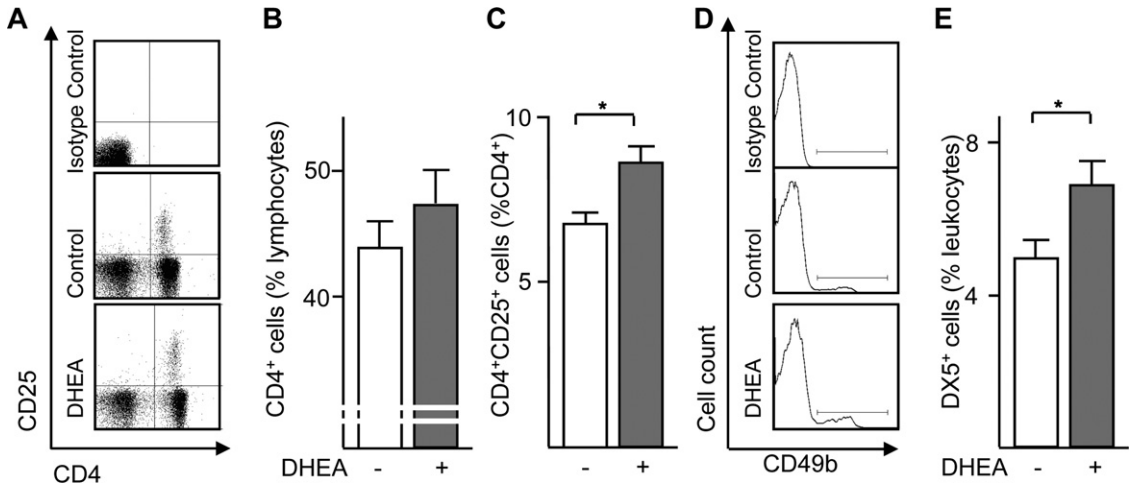

Fig. 5. Frequency of $CD4^+CD25^+$ and $DX5^+$ cells in peripheral blood. Representative dot plots from flow cytometric analysis of CD4 and CD25 positivity are displayed in (A). (B) Bars display the percentage of $CD4^+$ T cells and (C) activated ($CD4^+CD25^+$) cells among lymphocytes or $CD4^+$ cell population, respectively. (D) Representative histograms for $DX5^+$ NK cell identification by flow cytometry; (E) reveals the frequency of NK cells in blood leukocytes. Values shown in (B), (C) and (E) are mean ± SEM, $n = 5$ per group, $^*p < 0.05$, Mann–Whitney *U* test.

after an incubation period of 48 h, stimulation with DHEA resulted in an increased frequency of activated cells, as assessed by $CD25^+$. Interestingly, we observed that in this time point DHEA also induced the expression of VLA-4 and LFA-1 in activated $CD4^+$ and $CD8^+$ T cells (Supplementary Fig. 1B and Table 3), suggesting that DHEA not only induces the activation of T cells, but also their migration potential.

3.8. Evidence for follicular cyst infiltration by $CD4^+$ and $MHCII^+$ cells

Based on the above effects of DHEA on T cells, we further investigated the presence of $CD4^+$ T cells in the ovarian tissue by immunohistochemistry (IHC). In tissue sections from control and androgenised ovaries, the overall frequency of $CD4^+$ cells was very low. If present, $CD4^+$ cells could be localized in the theca cell layer of follicles, in the stromal tissue, and, rarely, in the granulosa cell layer and antrum of few developing follicles (Fig. 4M–P and Table 2). In ovaries from DHEA androgenised females, $CD4^+$ cells were also observed in the granulosa cell layer and antrum of all the cysts (Fig. 4P and Table 2).

Macrophages have been described to be the most abundant immune cell population in the ovary (Bukulmez and Arici, 2000; Wu et al., 2004). Thus, we evaluated the presence of macrophages – identified by MHCII – by IHC. Both in control and DHEA androgenised tissue we observed the presence of macrophages in the theca cell layer of follicles,

Table 3
Effect of *in vitro* stimulation with DHEA on lymphocyte subsets. Flow cytometric analysis of leukocytes upon stimulation with increasing concentrations of DHEA for 21 h or 48 h.

Frequency (%) of cell subsets/parental population[a]	*In vitro* stimulation of leukocytes with DHEA			
	Nil	0.1 μM	1 μM	10 μM
Stimulation for 21 h				
$CD3^+$/lymphocytes	73.9 ± 1.0	74.0 ± 1.2	73.1 ± 1.2	73.8 ± 1.0
$CD25^+/CD3^+$ cells	9.2 ± 0.4	9.4 ± 0.2	9.4 ± 0.3	9.3 ± 0.3
$CD4^+CD25^+/CD3^+$ cells	5.5 ± 0.3	5.4 ± 0.1	5.5 ± 0.3	5.5 ± 0.2
$CD4^+CD25^+$ VLA-$4^+/CD3^+$ cells	0.6 ± 0.0	0.6 ± 0.0	0.6 ± 0.0	0.6 ± 0.0
$CD4^+CD25^+$ LFA-$1^+/CD3^+$ cells	5.0 ± 0.2	4.9 ± 0.1	4.9 ± 0.2	4.8 ± 0.2
$CD8^+CD25^+/CD3^+$ cells	3.8 ± 0.1	4.0 ± 0.1	4.0 ± 0.1	3.7 ± 0.1
$CD8^+CD25^+$ VLA-$4^+/CD3^+$ cells	0.2 ± 0.0	0.2 ± 0.0	0.2 ± 0.0	0.2 ± 0.0
$CD8^+CD25^+$ LFA-$1^+/CD3^+$ cells	3.7 ± 0.1	3.8 ± 0.1	3.8 ± 0.1	3.6 ± 0.2
Stimulation for 48 h				
$CD3^+$/lymphocytes	76.8 ± 0.5	77.0 ± 0.5	76.9 ± 0.6	77.1 ± 0.6
$CD25^+/CD3^+$ cells	11.8 ± 0.5	**14.7 ± 0.6**	**15.4 ± 0.2**	**15.2 ± 0.8**
$CD4^+CD25^+/CD3^+$ cells	5.8 ± 0.3	**7.5 ± 0.4**	**7.8 ± 0.1**	**7.6 ± 0.4**
$CD4^+CD25^+$ VLA-$4^+/CD3^+$ cells	0.6 ± 0.1	**0.9 ± 0.1**	**0.9 ± 0.1**	**0.9 ± 0.3**
$CD4^+CD25^+$ LFA-$1^+/CD3^+$ cells	4.7 ± 0.2	**6.2 ± 0.3**	**6.2 ± 0.3**	**6.9 ± 0.5**
$CD8^+CD25^+/CD3^+$ cells	5.9 ± 0.2	**7.4 ± 0.2**	**7.5 ± 0.3**	**8.2 ± 0.9**
$CD8^+CD25^+$ VLA-$4^+/CD3^+$ cells	0.3 ± 0.0	**0.5 ± 0.1**	**0.5 ± 0.1**	**0.5 ± 0.0**
$CD8^+CD25^+$ LFA-$1^+/CD3^+$ cells	5.3 ± 0.2	**6.6 ± 0.2**	**6.7 ± 0.3**	**7.3 ± 0.8**

[a] Data are presented as mean frequency ± SEM in reference to the parental population. $n = 6$, numbers in bold indicate significant increase over Nil at $p < 0.05$, analysed by Mann–Whitney *U* test.

in the stromal tissue and, rarely, in the granulosa cell layer of follicles (Fig. 4I–L and Table 2). As it was reported in other animal models (Mannerås et al., 2007; Radavelli-Bagatini et al., 2011) we also detected macrophages in the granulosa cell layer and antrum of cysts (Fig. 4L and Table 2).

Interestingly, in androgenised ovaries ICAM$^+$, MHCII$^+$ and CD4$^+$ cells were present in the antrum and granulosa cell layer of the cysts especially near areas of high VCAM-1 expression (Fig. 4).

4. Discussion

PCOS is a complex endocrine disorder characterized by a deregulation of androgen synthesis (Escobar-Morreale and San Millán, 2007), anovulation and cyst formation (Rotterdam, 2004), often leading to infertility (Franks et al., 2008). Its association with metabolic disturbances, such as obesity, insulin resistance and chronic inflammation, has a significant impact on quality of life and possesses long term health risks for affected individuals (Hahn et al., 2005; Benson et al., 2007). We here provide evidence that experimentally induced hyperandrogenism in mice results in features similar to severe forms of PCOS in humans, as mice develop polycystic ovaries, anovulation, increased weight, insulin resistance and signs of chronic inflammation. Hence, we propose that DHEA-androgenisation serves as a good animal model towards a better understanding of the pathophysiology of PCOS in humans. Clearly, one limitation of the PCOS-mouse model using DHEA is that it does not allow conclusions about the pathogenesis of PCOS in humans, as PCOS-like symptoms are experimentally induced. Such a limitation is common in many mouse models of human disease. Regardless, pivotal insights can be teased apart using such models, as long as the limitations with regard to causality of diseases are respected.

We here describe a significant weight gain and insulin resistance as a result of DHEA-androgenisation in mice. These observations, along with data published by others (Eisner et al., 2003; Mannerås et al., 2007), indicate that androgens have a pivotal role on fat tissue metabolism and glucose and insulin homeostasis. DHEA androgenisation also induced an increase in the production of largely inflammatory cytokines and in the frequency of peripheral blood CD4$^+$CD25$^+$ and NK cells. These signs of chronic inflammation are similar to those observed in PCOS patients (Benson et al., 2007; Orio et al., 2005; Puder et al., 2005; Thomann et al., 2008). The interdependency of metabolic and inflammatory disorders is well documented in a number of studies, e.g. the secretion of adipokines by adipose tissue is compromised with the onset of insulin resistance and chronic inflammation in humans and rodents (Gambineri et al., 2002; Pasquali, 2006). Insulin resistance itself also contributes to chronic inflammation in PCOS (Orio et al., 2005). Conversely, chronic inflammation enhances insulin resistance, emphasizing the vicious cycle of metabolic disorders in PCOS. Further, immune cells can be affected directly by androgens, as revealed by our *in vitro* results. Taken together, our data highlight the importance of androgens in triggering both metabolic disorders and inflammation. Clearly, the co-occurrence of these features of PCOS in androgenised mice does not imply causality, but provides a lead to test pathways or redundancies of certain markers in future research endeavours.

We further describe that DHEA-androgenisation resulted in the formation of follicular cysts in mouse ovaries, which appeared at a higher frequency when treatment was started at a younger age. This could be related to the early onset of PCOS in humans (Ibanez et al., 2006). Like in human PCOS, ovarian cysts occur along with anovulation and an altered ovarian steroidogenesis, as revealed by the estrous cycle arrest and increased levels of serum estradiol. High levels of estradiol have been observed in polycystic women (Codner et al., 2007), particularly when undergoing hormonal treatment for IVF (Suikkari et al., 1995). The ovarian dysfunction is known to be an ultimate result of hyperandrogenism, e.g. in the animal model we employed, but also in experimental models, e.g. using testosterone (Mannerås et al., 2007) or in human hyperandrogenic disorders such as PCOS. Insulin can potentiate ovarian pathologies, i.e. by triggering similar pathways as gonadotropins to stimulate ovarian steroidogenesis (Young and McNeilly, 2010). Accordingly, improvement of insulin sensitivity in PCOS, i.e. by the anti-hyperglucaemic drug metformin, often restores ovulation in PCOS (Johnson, 2011) and improves ovarian related parameters in DHEA androgenised mice (Sander et al., 2006). Hence, future research should unveil if and how metformin treatment affects PCOS-related inflammatory symptoms in DHEA-treated mice.

We further observed an increased frequency of CD4$^+$ cells in the granulosa cell layer and antrum of cysts, along with a large number of MHCII$^+$ cells. In the ovary, CD4$^+$ T helper cells and macrophages, through the secretion of cytokines, metalloproteinases and other inflammatory mediators, orchestrate tissue remodelling and apoptosis, both of which are involved in folliculogenesis, ovulation and CL formation (Wu et al., 2004). In healthy antral follicles, leukocytes are excluded from the granulosa cells and antral compartment by the basal membrane (Irving-Rodgers et al., 2009). Interestingly, T helper cells have been previously described in ovarian follicles of PCOS women (Gallinelli et al., 2003), though their function remains unknown. Similarly, peripheral blood CD4$^+$ T cells also increased after DHEA androgenisation in the model we describe here. This suggests that androgenisation acts through specific receptors on T cells. It has been proposed that CD4$^+$ T cells express a receptor for DHEA (Meikle et al., 1992). Further, androgenisation may act through estrogen receptors present on T cells (Komesaroff, 2008). Our *in vitro* data support a direct effect of DHEA on CD4$^+$ T cells. Moreover, we observed that DHEA androgenisation *in vitro* promotes the expression of the integrins VLA-4 and LFA-1 on CD4$^+$ T cells. Upon activation, these molecules can bind VCAM-1 and ICAM-1, respectively (Blois et al., 2005).

Thus, in the present work, we describe an up-regulation of both CAMs in the granulosa cell layer of cysts. Further, VCAM-1 was highly expressed in the theca cell layer of all ovarian follicles and cysts in DHEA-androgenised animals. The up-regulation of VCAM-1 and ICAM-1 could be a result of systemic hyperinsulinemia and inflammation, since insulin and inflammatory cytokines have previously been reported to up-regulate the expression of these CAMs

(Blois et al., 2005; Madonna et al., 2008). Strikingly, in healthy ovaries, the expression of CAMs has been shown to be under the regulation of the estrous cycle, which in turn controls the ovarian homing of immune cells from blood (Bonello et al., 2004; Katayama et al., 2003). We observed that upon DHEA treatment in mice, the expression of VCAM-1 and ICAM-1 was up-regulated particularly in the granulosa cell layer of cysts, along with the spatial accumulation of leukocytes. This observation suggests that the up-regulation of adhesion molecules in ovarian follicles facilitates cellular migration into the ovary in androgenised mice. We envision that multiple processes are engaged in the ovarian homing of cells, which include the enhanced expression of CAMs in the ovary promoting cell migration as well as the increased frequency of circulating activated $CD4^+$ T cells co-expressing ligands for CAMs. Thus, it is tempting to speculate that the enhanced migration of $CD4^+$ T cells – possibly along with MHC II^+ activated macrophages – to the ovaries accounts for increased granulosa cell layer epithelialization and tissue remodelling, ultimately leading to cyst formation and anovulation.

Further experiments are required to evaluate this hypothesis. The lack of viable mice lacking VCAM-1 and ICAM-1 – which could otherwise provide insight on the biological importance of CAMs in PCOS – limits the possibility of testing the DHEA model in the presence or absence of these CAMs. However, blockage of VCAM-1 gene expression can be achieved by the administration of the antioxidant drug succinobucol (AGI-1067), among other agents (Stocker, 2009). Interestingly, succinobucol has been proven to be beneficial for diseases with inflammatory components, such as diabetes and atherosclerosis (Crim et al., 2010; Preiss and Sattar, 2007; Tardif et al., 2008). This suggests that blockage of VCAM-1 could constitute a potential therapeutic target in PCOS. The soluble form of VCAM-1 (sVCAM-1) has been detected in follicular fluid of women undergoing IVF where its levels correlated positively to progesterone levels (Fornaro et al., 2007), fertilization rate, the degree of theca cell layer luteinization, levels of vascular endothelial growth factor (Benifla et al., 2001) and angiogenic effects in late follicular developmental stages (Gruemmer et al., 2005). Taken together, these data allow us to speculate that abnormal expression of VCAM-1 in the ovary of androgenised mice could be related not only to leukocyte migration to cysts but also to the altered angiogenesis, theca cell layer function, and follicular development described in polycystic ovaries (Hughesdon, 1982; Järvelä et al., 2004; Webber et al., 2007). Thus, the availability of this well characterized DHEA-induced mouse model mimicking the disease in humans may now serve as a tool to further dissect the inter-relationships of clinical features in PCOS.

Acknowledgements

The experimental work presented herein was made possible by grants provided by the Banting Foundation and the Charité. MES was awarded with a scholarship from the German Academic Exchange Program (DAAD). The authors wish to thank Evelin Hagen and Petra Busse for their technical support, Dr. Khalil Karimi for his suggestions with regard to the experimental design and helpful discussion, and Caitlin Jago for her assistance in writing the manuscript.

Appendix A. Supplementary data

Supplementary data associated with this article can be found, in the online version, at doi:10.1016/j.jri.2011.09.003.

References

Abbott, D.H., Barnett, D.K., Bruns, C.M., Dumesic, D.A., 2005. Androgen excess fetal programming of female reproduction: a developmental aetiology for polycystic ovary syndrome? Hum. Reprod. Update 11, 357–374.

Amato, G., Conte, M., Mazziotti, G., Lalli, E., Vitolo, G., Tucker, A.T., et al., 2003. Serum and follicular fluid cytokines in polycystic ovary syndrome during stimulated cycles. Obstet. Gynecol. 101, 1177–1182.

Andrikopoulos, S., Blair, A.R., Deluca, N., Fam, B.C., Proietto, J., 2008. Evaluating the glucose tolerance test in mice. Am. J. Physiol. Endocrinol. Metab. 295, 1323–1332.

Azziz, R., Woods, K.S., Reyna, R., Key, T.J., Knochenhauer, E.S., Yildiz, B.O., 2004. The prevalence and features of the polycystic ovary syndrome in an unselected population. J. Clin. Endocrinol. Metab. 89, 2745–2749.

Asuncion, M., Calvo, R.M., San Millan, J.L., Sancho, J., Avila, S., Escobar-Morreale, H.F., 2000. A prospective study of the prevalence of the polycystic ovary syndrome in unselected Caucasian women from Spain. J. Clin. Endocrinol. Metab. 85, 2434–2438.

Bas, D., Abramovich, D., Hernandez, F., Tesone, M., 2011. Altered expression of Bcl-2 and Bax in follicles within dehydroepiandrosterone-induced polycystic ovaries in rats. Cell Biol. Int. 35, 423–429.

Berglund, E.D., Li, C.Y., Poffenberger, G., Ayala, J.E., Fueger, P.T., Willis, S.E., et al., 2008. Glucose metabolism in vivo in four commonly used inbred mouse strains. Diabetes 57, 1790–1799.

Benifla, J.L., Bringuier, A.F., Sifer, C., Porcher, R., Madelenat, P., Feldmann, G., 2001. Vascular endothelial growth factor, platelet endothelial cell adhesion molecule-1 and vascular cell adhesion molecule-1 in the follicular fluid of patients undergoing IVF. Hum. Reprod. 16, 1376–1381.

Benson, S., Janssen, O.E., Hahn, S., Tan, S., Dietz, T., Mann, K., et al., 2007. Obesity, depression, and chronic low-grade inflammation in women with polycystic ovary syndrome. Brain Behav. Immun. 22, 177–184.

Bonello, N., Jasper, M.J., Norman, R.J., 2004. Periovulatory expression of intercellular adhesion molecule-1 in the rat ovary. Biol. Reprod. 71, 1384–1390.

Blois, S., Tometten, M., Kandil, J., Hagen, E., Klapp, B.F., Margni, R.A., et al., 2005. Intercellular adhesion molecule-1/LFA-1 cross talk is a proximate mediator capable of disrupting immune integration and tolerance mechanism at the feto-maternal interface in murine pregnancies. J. Immunol. 74, 1820–1829.

Brannstrom, M., Norman, R.J., 1993. Involvement of leukocytes and cytokines in the ovulatory process and corpus luteum function. Hum. Reprod. 8, 1762–1775.

Brüünsgaard, H., Pedersen, B.K., 2003. Age-related inflammatory cytokines and disease. Immunol. Allergy Clin. North Am. 23, 15–39.

Bukulmez, O., Arici, A., 2000. Leukocytes in ovarian function. Hum. Reprod. Update 6, 1–15.

Cheng, G., Weihua, Z., Mäkinen, S., Mäkelä, S., Saji, S., Warner, M., et al., 2002. A role for the androgen receptor in follicular atresia of estrogen receptor beta knockout mouse ovary. Biol. Reprod. 66, 77–84.

Codner, E., Iñíguez, G., Villarroel, C., Lopez, P., Soto, N., Sir-Petermann, T., et al., 2007. Hormonal profile in women with polycystic ovarian syndrome with or without type 1 diabetes mellitus. J. Clin. Endocrinol. Metab. 92, 4742–4746.

Crim, W.S., Wu, R., Carter, J.D., Cole, B.K., Trace, A.P., Mirmira, R.G., et al., 2010. AGI-1067, a novel antioxidant and anti-inflammatory agent, enhances insulin release and protects mouse islets. Mol. Cell. Endocrinol. 323, 246–255.

Diamanti-Kandarakis, E., Kouli, C.R., Bergiele, A.T., Filandra, F.A., Tsianateli, T.C., Spina, G.G., et al., 1999. A survey of the polycystic ovary syndrome in the Greek island of Lesbos: hormonal and metabolic profile. J. Clin. Endocrinol. Metab. 84, 4006–4011.

Diamanti-Kandarakis, E., Alexandraki, K., Piperi, C., Protogerou, A., Katsikis, I., Paterakis, T., 2006. Inflammatory and endothelial markers in women with polycystic ovary syndrome. Eur. J. Clin. Invest. 36, 691–697.

Eisner, J.R., Dumesic, D.A., Kemnitz, J.W., Colman, R.J., Abbott, D.H., 2003. Increased adiposity in female rhesus monkeys exposed to androgen excess during early gestation. Obes. Res. 11, 279–286.

Escobar-Morreale, H.F., San Millán, J.L., 2007. Abdominal adiposity and the polycystic ovary syndrome. Trends Endocrinol. Metab. 18, 266–272.

Escobar-Morreale, H.F., Villuendas, G., Botella-Carretero, J.I., Sancho, J., San Millan, J.L., 2003. Obesity, and not insulin resistance, is the major determinant of serum inflammatory cardiovascular risk markers in pre-menopausal women. Diabetologia 46, 625–633.

Fornaro, F., Cobellis, L., Mele, D., Tassou, A., Badolati, B., Sorrentino, S., et al., 2007. Effects of gonadotropin-releasing hormone agonist/recombinant follicle-stimulating hormone versus gonadotropin-releasing hormone antagonist/recombinant follicle-stimulating hormone on follicular fluid levels of adhesion molecules during in vitro fertilization. Fertil. Steril. 87, 39–47.

Franks, S., Strak, J., Hardy, K., 2008. Follicle dynamics and anovulation in polycystic ovary syndrome. Hum. Reprod. Update 14, 367–378.

Gallinelli, A., Ciaccio, I., Giannella, L., Salvatori, M., Marsella, T., Volpe, A., 2003. Correlations between concentrations of interleukin-12 and interleukin-13 and lymphocyte subsets in the follicular fluid of women with and without polycystic ovary syndrome. Fertil. Steril. 79, 1365–1372.

Gambineri, A., Pelusi, C., Vicennati, V., Pagotto, U., Pasquali, R., 2002. Obesity and the polycystic ovary syndrome. Int. J. Obes. Relat. Metab. Disord. 26, 883–896.

Goodarzi, M.O., Dumesic, D.A., Chazenbalk, G., Azziz, R., 2011. Polycystic ovary syndrome: etiology, pathogenesis and diagnosis. Nat. Rev. Endocrinol. 7, 219–231.

Gruemmer, R., Klein-Hitpaß, L., Neulen, J., 2005. Regulation of gene expression in endothelial cells: the role of human follicular fluid. J. Mol. Endocrinol. 34, 37–46.

Hahn, S., Tan, S., Elsenbruch, S., Quadbeck, B., Herrmann, B.L., Mann, K., et al., 2005. Clinical and biochemical characterization of women with polycystic ovary syndrome in North Rhine-Westphalia. Horm. Metab. Res. 37, 438–444.

Hughesdon, P.E., 1982. Morphology and morphogenesis of the Stein-Leventhal ovary and of so-called 'hyperthecosis'. Obstet. Gynecol. Surv. 37, 59–77.

Ibanez, L., Valls, C., Ong, K., Dunger, D.B., de Zegher, F., 2006. Metformin therapy during puberty delays menarche. prolongs pubertal growth, and augments adult height: a randomized study in low-birth-weight girls with early-normal onset of puberty. J. Clin. Endocrinol. Metab. 91, 2068–2073.

Irving-Rodgers, H.F., Morris, S., Collett, R.A., Peura, T.T., Davy, M., Thompson, J.G., et al., 2009. Phenotypes of the ovarian follicular basal lamina predict developmental competence of oocytes. Hum. Reprod. 24, 936–944.

Henmi, H., Endo, T., Nagasawa, K., Hayashi, T., Chida, M., Akutagawa, N., et al., 2001. Lysyl oxidase and MMP-2 expression in dehydroepiandrosterone-induced polycystic ovary in rats. Biol. Reprod. 64, 157–162.

Jansen, E., Laven, J.S., Dommerholt, H.B., Polman, J., van Rijt, C., van den Hurk, C., et al., 2004. Abnormal gene expression profiles in human ovaries from polycystic ovary syndrome patients. Mol. Endocrinol. 18, 3050–3063.

Järvelä, I.Y., Sladkevicius, P., Kelly, S., Ojha, K., Campbell, S., Nargund, G., 2004. Comparison of follicular vascularization in normal versus polycystic ovaries during in vitro fertilization as measured using 3-dimensional power Doppler ultrasonography. Fertil. Steril. 82, 1358–1363.

Johnson, N., 2011. Metformin is a reasonable first-line treatment option for non-obese women with infertility related to anovulatory polycystic ovary syndrome—a meta-analysis of randomised trials. Aust. N. Z. J. Obstet. Gynaecol. 51, 125–129.

Katayama, T., Kusanagi, Y., Kiyomura, M., Ochi, H., Ito, M., 2003. Leukocyte behaviour and permeability in the rat mesenteric microcirculation following induction of ovulation. Hum. Reprod. 18, 1179–1184.

Knochenhauer, E.S., Key, T.J., Kahsar-Miller, M., Waggoner, W., Boots, L.R., Azziz, R., 1998. Prevalence of the polycystic ovary syndrome in unselected black and white women of the southeastern United States: a prospective study. J. Clin. Endocrinol. Metab. 83, 3078–3082.

Komesaroff, P.A, 2008. Unravelling the enigma of dehydroepiandrosterone: moving forward step by step. Endocrinology 149, 886–888.

Lee, G.Y., Croop, J.M., Anderson, E., 1998. Multidrug resistance gene expression correlates with progesterone production in dehydroepiandrosterone-induced polycystic and equine chorionic gonadotropin-stimulated ovaries of prepubertal rats. Biol. Reprod. 58, 330–337.

Lee, M., Anderson, E., Lee, G.Y., 1991. Changes in ovarian morphology and serum hormones in the rat after treatment with dehydroepiandrosterone. Anat. Rec. 231, 185–192.

Luchetti, C.G., Solano, M.E., Sander, V., Barreiro Arcos, M.L., Gonzalez, C., Di Girolamo, G., et al., 2004. Effects of dehydroepiandrosterone on ovarian cystogenesis and immune function. J. Reprod. Immunol. 64, 59–74.

Maciel, G.A., Baracat, E.C., Benda, J.A., Markham, S.M., Hensinger, K., Chang, R.J., et al., 2004. Stockpiling of transitional and classic primary follicles in ovaries of women with polycystic ovary syndrome. J. Clin. Endocrinol. Metab. 89, 5321–5327.

Madonna, R., Massaro, M., De Caterina, R., 2008. Insulin potentiates cytokine-induced VCAM-1 expression in human endothelial cells. Biochim. Biophys. Acta 1782, 511–516.

Mannerås, L., Cajander, S., Holmäng, A., Seleskovic, Z., Lystig, T., Lönn, M., et al., 2007. A new rat model exhibiting both ovarian and metabolic characteristics of polycystic ovary syndrome. Endocrinology 148 (8), 3781–3791.

Martinez-Bermejo, E., Luque-Ramirez, M., Escobar-Morreale, H.F., 2007. Obesity and the polycystic ovary syndrome. Minerva Endocrinol. 32, 129–140.

Meikle, A.W., Dorchuck, R.W., Araneo, B.A., Stringham, J.D., Evans, T.G., Spruance, S.L., et al., 1992. The presence of a dehydroepiandrosterone-specific receptor binding complex in murine T cells. J. Steroid Biochem. Mol. Biol. 42, 293–304.

Meyer, C., McGrath, B.P., Teede, H.J., 2005a. Overweight women with polycystic ovary syndrome have evidence of subclinical cardiovascular disease. J. Clin. Endocrinol. Metab. 90, 5711–5716.

Meyer, C., McGrath, B.P., Cameron, J., Kotsopoulos, D., Teede, H.J., 2005b. Vascular dysfunction and metabolic parameters in polycystic ovary syndrome. J. Clin. Endocrinol. Metab. 90, 4630–4635.

Möhlig, M., Spranger, J., Osterhoff, M., Ristow, M., Pfeiffer, A.F., Schill, T., et al., 2004. The polycystic ovary syndrome per se is not associated with increased chronic inflammation. Eur. J. Endocrinol. 150, 525–532.

Muniyappa, R., Lee, S., Chen, H., Quoan, M.J., 2008. Current approaches for assessing insulin sensitivity and resistance in vivo: advantages, limitations, and appropriate usage. Am. J. Physiol. Endocrinol. Metab. 294, 15–26.

Omu, A.E., Al-Azemi, M.K., Makhseed, M., Al-Oattan, F., Ismail, A.A., Al-Tahir, S., et al., 2003. Differential expression of T-helper cytokines in the peritoneal fluid of women with normal ovarian cycle compared with women with chronic anovulation. Acta Obstet. Gynecol. Scand. 82, 603–609.

Orio Jr., F., Palomba, S., Cascella, T., Di Biase, S., Manguso, F., Tauchmanovà, L., et al., 2005. The increase of leukocytes as a new putative marker of low-grade chronic inflammation and early cardiovascular risk in polycystic ovary syndrome. J. Clin. Endocrinol. Metab. 90, 2–5.

Pasquali, R., Stener-Victorin, E., Yildiz, B.O., Duleba, A.J., Hoeger, K., Mason, H., et al., 2011. PCOS forum: research in polycystic ovary syndrome today and tomorrow. Clin. Endocrinol. (Oxf.) 74, 424–433.

Pasquali, R., 2006. Obesity and androgens: facts and perspectives. Fertil. Steril. 85, 1319–1340.

Prados, M.B., Solano, M.E., Friebe, A., Blois, S., Arck, P., Miranda, S., 2011. Stress increases VCAM-1 expression at the fetomaternal interface in an abortion-prone mouse model. J. Reprod. Immunol. 89, 207–211.

Preiss, D.J., Sattar, N., 2007. Vascular cell adhesion molecule-1: a viable therapeutic target for atherosclerosis? Int. J. Clin. Pract. 61, 697–701.

Puder, J.J., Varga, S., Kraenzlin, M., De Geyter, C., Keller, U., Müller, B., 2005. Central fat excess in polycystic ovary syndrome: relation to low-grade inflammation and insulin resistance. J. Clin. Endocrinol. Metab. 90, 6014–6021.

Radavelli-Bagatini, S., Blair, A.R., Proietto, J., Spritzer, P.M., Andrikopoulos, S., 2011. The New Zealand obese mouse model of obesity insulin resistance and poor breeding performance: evaluation of ovarian structure and function. J. Endocrinol. 209, 307–315.

Rotterdam ESHRE/ASRM-Sponsored PCOS Conference Workshop Group, 2004. Revised 2003 consensus on diagnostic criteria and long-term health risks related to polycystic ovary syndrome. Fertil. Steril. 81, 19–25.

Roy, S., Mahesh, V.B., Greenblatt, R.B., 1962. Effect of dehydroepiandrosterone and androstenedione on the reproductive organs of female rats: production of cystic changes in the ovary. Nature 196, 2–6.

Sander, V., Luchetti, C.G., Elia, E., Solano, M.E., Di Girolamo, G., Gonzalez, C., et al., 2006. Role of the N,N′-dimethylbiguanide metformin in the treatment of female prepuberal BALB/c mice hyperandrogenized with dehydroepiandrosterone. Reproduction 131, 591–602.

Sander, V.A., Piehl, L., Facorro, G.B., Rubín de Celis, E., Motta, A.B., 2008. Regulation of functional and regressing stages of corpus luteum development in mice. Role of reactive oxygen species. Reprod. Fertil. Dev. 20, 760–769.

Sayin, N.C., Gücer, F., Balkanli-Kaplan, P., Yüce, M.A., Ciftci, S., Kücük, M., et al., 2003. Elevated serum TNF-alpha levels in normal-weight women with polycystic ovaries or the polycystic ovary syndrome. J. Reprod. Med. 48, 165–170.

Stocker, R., 2009. Molecular mechanisms underlying the antiatherosclerotic and antidiabetic effects of probucol, succinobucol, and other probucol analogues. Curr. Opin. Lipidol. 20, 227–235.

Suikkari, A.M., McLachlan, V., Montalto, J., Calderon, I., Healy, D.L., McLachlan, R.I., et al., 1995. Ultrasonographic appearance of polycystic ovaries is associated with exaggerated ovarian androgen and oestradiol responses to gonadotrophin-releasing hormone agonist in women undergoing assisted reproduction treatment. Hum. Reprod. 10, 513–519.

Tardif, J.C., Grégoire, J., L'Allier, P.L., Ibrahim, R., Anderson, T.J., Reeves, F., et al., 2008. Effects of the antioxidant succinobucol (AGI-1067) on human atherosclerosis in a randomized clinical trial. Atherosclerosis 197, 480–486.

Thomann, R., Rossinelli, N., Keller, U., Tirri, B.F., De Geyter, C., Ruiz, J., et al., 2008. Differences in low-grade chronic inflammation and insulin resistance in women with previous gestational diabetes mellitus and women with polycystic ovary syndrome. Gynecol. Endocrinol. 24, 199–206.

Webber, L.J., Stubbs, S.A., Stark, J., Margara, R.A., Trew, G.H., Lavery, S.A., et al., 2007. Prolonged survival in culture of preantral follicles from polycystic ovaries. J. Clin. Endocrinol. Metab. 92, 1975–1978.

Wu, R., Fujii, S., Ryan, N.K., Van der Hoek, K.H., Jasper, M.J., Sini, I., 2007. Ovarian leukocyte distribution and cytokine/chemokine mRNA expression in follicular fluid cells in women with polycystic ovary syndrome. Hum. Reprod. 22, 527–535.

Wu, R., Van der Hoek, K.H., Ryan, N.K., Norman, R.J., Robker, R.L., 2004. Macrophage contributions to ovarian function. Hum. Reprod. Update 10, 119–133.

Yan, Z., Lee, G.Y., Anderson, E., 1997. Influence of dehydroepiandrosterone on the expression of insulin-like growth factor-1 during cystogenesis in polycystic rat ovaries and in cultured rat granulosa cells. Biol. Reprod. 57, 1509–1516.

Young, J.M., McNeilly, A.S., 2010. Theca: the forgotten cell of the ovarian follicle. Reproduction 140, 489–504.